

From Cylinders to Helices upon Confinement

Hongqi Xiang, Kyusoon Shin, Taehyung Kim,
Sung In Moon, Thomas J. McCarthy, and
Thomas P. Russell*

Polymer Science and Engineering Department, University of
Massachusetts, Amherst, Massachusetts 01003

Received November 19, 2004

Revised Manuscript Received January 3, 2005

Confinement can break the symmetry of a structure, forcing a change from bulk equilibrium behavior. Diblock copolymers, with their rich phase behavior and ordering transitions, are ideally suited to study structural transitions arising from confinement.¹ The self-assembly of symmetric block copolymers under a one-dimensional confinement, imposed by two parallel bounding surfaces, has been extensively studied both theoretically and experimentally.^{2–13} Recently, we investigated the two-dimensional confinement of symmetric diblock copolymers of styrene and butadiene, PS-*b*-PBD, using nanoscopic cylindrical pores in alumina membranes.^{14,15} In the bulk this copolymer exhibits a lamellar microdomain morphology. Within the pores, the symmetric PS-*b*-PBD copolymers show a multiple set of concentric cylinders, when the pore diameter, d , is large in comparison to the equilibrium period, L_0 .^{14,16,17} However, as the pore diameter decreases, becoming comparable to L_0 , and when d/L_0 is not an integer, a novel stacked-disk or torroid type of morphology forms in the pores.¹⁵

We report here the phase behavior of a cylinder-forming diblock copolymer under similar confinement. A helical morphology is found to form under certain conditions. This nanostructured material is interesting for its potential applications in fabricating unique nanostructured materials from diblock copolymers, expanding the types of morphology accessible from these simple molecules.

The PS-*b*-PBD copolymer used in this study (Polymer Sources) had a number-average molecular weight of 42 000 and a polydispersity index of 1.03 with a volume fraction of ~ 0.36 PBD. The bulk morphology consists of PBD cylinders in a PS matrix with $L_0 \sim 29.1$ nm, as measured by small-angle X-ray scattering (SAXS). The alumina membranes were electrochemically prepared in 0.3 M oxalic acid by a two-step anodization process.¹⁸ The nanopores formed in the alumina membranes were 33–45 nm in diameter with a length of ~ 5 μm . To confine the copolymer in the cylindrical nanopores, the alumina membrane was placed on top of a dried PS-*b*-PBD film that was solvent-cast onto a glass slide. The assembly was heated to 125 °C under vacuum, and the copolymer melt was drawn into the nanopores by capillary force. After annealing for 7 days, the copolymer/membrane assembly was allowed to cool to room temperature. The alumina membrane was removed using a 5% (w/w) sodium hydroxide solution (water/methanol: 8:2 by volume), leaving an array of free-standing copolymer nanorods. To visualize the microphase-separated morphology in the copolymer nanorods, transmission electron microscopy (TEM) was used. For this

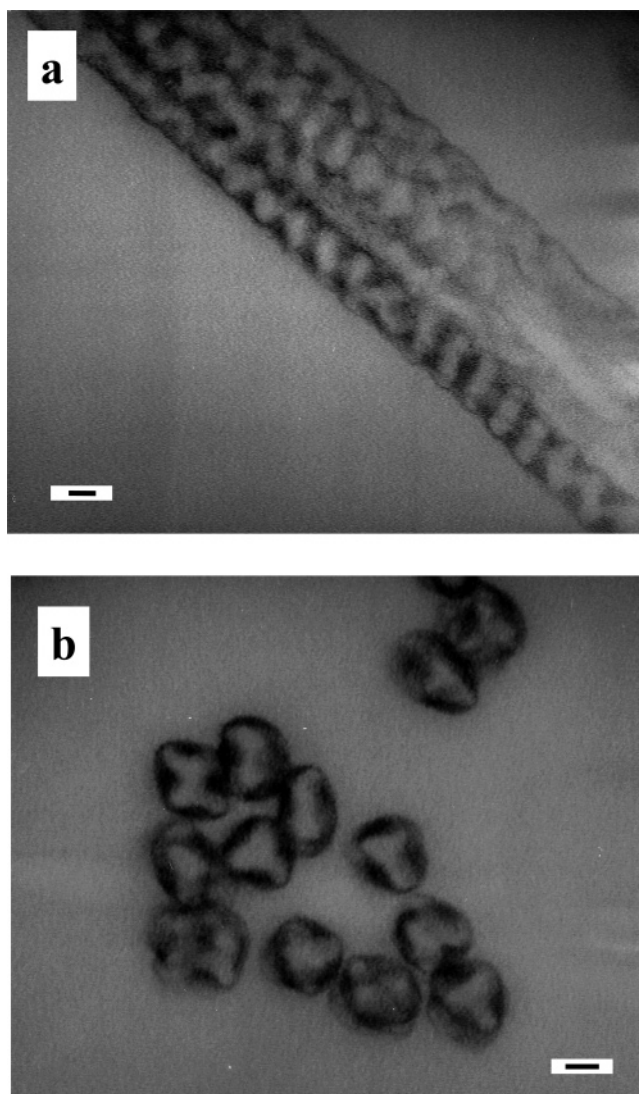


Figure 1. TEM images of PS-*b*-PBD nanorods prepared using anodic alumina membranes: (a) cross-sectional view along the axes of the nanorods (three shown in the image); (b) cross-sectional view normal to the axes of the rods. Each circular cross section represents a cut across one nanorod showing cross sections of the morphology in each nanorod. Approximately 14 cross sections are shown in this image. The scale bars in the two images are 20 nm.

purpose, the nanorods were embedded in an epoxy resin and microtomed parallel and normal to the rod axis. The as-prepared ultrathin sections were exposed to OsO₄, which preferentially stained the PBD phase.

PS and PBD are highly immiscible, and PBD, having the lower surface energy, preferentially segregates to the high-surface-energy alumina interface. Previous studies showed that,¹⁴ in nanopores with diameters d larger than ~ 120 nm ($d/L_0 > 4.1$), the hexagonal packing of the cylindrical domains is maintained, but both the symmetry and separation distance of the hexagonal packing can be altered by the shape and size of the pores. For a pore diameter ~ 120 nm, only seven cylinders are formed within the pore. Shown in Figure 1a is a cross-sectional TEM image along the axis of the cylindrical PS-*b*-PBD nanorods confined in pores with diameters of 33–45 nm ($d/L_0 = 1.1$ – 1.5). Within the

* To whom correspondence should be addressed: Tel 413-545-2680; Fax 413-577-1510; e-mail russell@mail.pse.umass.edu.

nanorods, the microphase-separated morphology of the copolymer is well-developed. The lower surface energy PBD domain (dark regions) is located at the pore walls, highlighting the edges of the nanorods. However, the alignment of cylindrical domains along the rod axis, which occurs when $d/L_0 > 4.1$, is no longer observed. Rather, dark lines are seen at a constant angle with respect to the nanorod axis, indicating that PBD forms a helical structure, while maintaining contact with the pore walls. The pitch of the helix is $\sim 18^\circ$ with an ~ 30 nm period, quite close to L_0 . Figure 1b shows a TEM image normal to the nanorod axis of the PS-*b*-PBD prepared in 33–45 nm diameter pores. The cross-section structure consists of only two domains, PS at center and PBD ring outside. Two to four small PBD protrusions into the central PS core are seen, evenly distributed around the PS center. This indicates that, depending on d/L_0 , multiple helices are formed. In the bulk, the morphology consists of PBD cylinders in a PS matrix. Within the nanopores, PBD adsorbs to the curved walls of the alumina pores, forcing the opposite curvature on the PS domain. There also appears to be a discrepancy in the volume fraction of the PBD determined from the TEM image compared to the actual value. This arises from the projection of the morphology onto a plane when obtaining the TEM image. TEM measurements obtained at different tilt angles of the sample are currently underway to quantify this structure. It is clear, though, that the morphology has changed from simple cylinders oriented along the axis of the nanorods to a morphology where the cylinders form helices within the nanopores.

Elbs et al.^{19,20} observed a similar type of morphological transition in thin films of ABC triblock copolymers. With slight changes in film thickness, a transition in the morphology from concentric cylinders of the A and B microdomains in a C matrix converted into helices of B microdomains around a central A core in a C matrix was observed. Recently, Wu et al. observed the formation of helical and torroid-like structure in a silica surfactant system confined within similar alumina membranes.²¹ Upon calcining, exquisite silica structures were found by TEM. Theoretical arguments were used to describe the observed structures in these complex, multicomponent systems. The results shown in this study, along with those of Wu et al.²¹ and results from our previous study,^{14,15} speak to the generality of confinement-induced structure transitions which ex-

pand the repertoire of nanoscopic block copolymer scaffolds.

Acknowledgment. This work was supported by the National Science Foundation through the Materials Research Science and Engineering Center (DMR-0213695) and the Nanoscience Interdisciplinary Research Team (DMR-0103024) at the University of Massachusetts, Amherst, the U.S. Department of Energy, Office of Basic Energy Sciences (DE-FG02-96ER45612), and Hyperstructured Organic Materials Research Center supported by the Korea Science Foundation.

References and Notes

- (1) Bates, F. S.; Frederickson, G. H. *Annu. Rev. Phys. Chem.* **1990**, *41*, 525.
- (2) Turner, M. S. *Phys. Rev. Lett.* **1992**, *69*, 1788.
- (3) Shull, K. R. *Macromolecules* **1992**, *25*, 2122.
- (4) Kikuchi, M.; Binder, K. *Europhys. Lett.* **1993**, *21*, 427.
- (5) Walton, D. G.; Kellogg, G. J.; Mayes, A. M.; Lambooy, P.; Russell, T. P. *Macromolecules* **1994**, *27*, 6225.
- (6) Lambooy, P.; Russell, T. P.; Kellogg, G. J.; Mayes, A. M.; Gallagher, P. D.; Satija, S. K. *Phys. Rev. Lett.* **1994**, *72*, 2899.
- (7) Brown, G.; Chakrabarti, A. *J. Chem. Phys.* **1995**, *102*, 1440.
- (8) Koneripalli, N.; Singh, N.; Levicky, R.; Bates, F. S.; Gallagher, P. D.; Satija, S. K. *Macromolecules* **1995**, *28*, 2897.
- (9) Kellogg, G. J.; Walton, D. G.; Mayes, A. M.; Lambooy, P.; Russell, T. P.; Gallagher, P. D.; Satija, S. K. *Phys. Rev. Lett.* **1996**, *76*, 2503.
- (10) Matsen, M. W. *J. Chem. Phys.* **1997**, *106*, 7781.
- (11) Pickett, G.; Balazs, A. C. *Macromol. Theory Simul.* **1998**, *7*, 249.
- (12) Fasolka, M. J.; Banerjee, P.; Mayes, A. M.; Pickett, G.; Balazs, A. C. *Macromolecules* **2000**, *33*, 5702.
- (13) Tang, W. H. *Macromolecules* **2000**, *33*, 1370.
- (14) Xiang, H.; Shin, K.; Kim, T.; Moon, S. I.; McCarthy, T. J.; Russell, T. P. *Macromolecules* **2004**, *37*, 3660.
- (15) Shin, K.; Xiang, H.; Moon, S. I.; Kim, T.; McCarthy, T. J.; Russell, T. P. *Science* **2004**, *306*, 76.
- (16) He, X.-H.; Song, M.; Liang, H.-J.; Pan, C.-Y. *J. Chem. Phys.* **2001**, *114*, 10510.
- (17) Sevink, G. J. A.; Zvelindovsky, A. V.; Fraaije, J. G. E. M.; Huinink, H. P. *J. Chem. Phys.* **2001**, *115*, 8226.
- (18) Masuda, H.; Fukuda, K. *Science* **1995**, *268*, 1466.
- (19) Elbs, H.; Abetz, V.; Hadziioannou, G.; Drummer, C.; Krausch, G. *Macromolecules* **2001**, *34*, 7917.
- (20) Elbs, H.; Drummer, C.; Abetz, V.; Krausch, G. *Macromolecules* **2002**, *35*, 5570.
- (21) Wu, Y.; Cheng, G.; Katsov, K.; Sides, S. W.; Wang, J.; Tang, J.; Fredrickson, G. H.; Moskovits, M.; Stucky, G. D. *Nat. Mater.* **2004**, *3*, 816.

MA0476036